From ZIF-8@Al_2O_3 Composites to Self-Supported ZIF-8 One-Dimensional Superstructures

Marion Gualino,[†,‡] Nans Roques,[*,†,‡] Stéphane Brandès,[§] Laurent Ararault,[∥] and Jean-Pascal Sutter[*,†,‡]

[†]CNRS, LCC (Laboratoire de Chimie de Coordination), 205 route de Narbonne, F-31077 Toulouse, France

[‡]Université de Toulouse, UPS, INPT, F-31077 Toulouse Cedex 4, France

[§]ICMUB (Institut de Chimie Moléculaire de l'Université de Bourgogne), UMR 6302 CNRS, Université de Bourgogne Franche-Comté, F-21078, Dijon, France

[∥]Université de Toulouse ; CIRIMAT, UPS/INPT/CNRS, LCMIE, 118 route de Narbonne, F-31062 Toulouse, France

S *Supporting Information*

ABSTRACT: Efficient preparation of composite materials consisting of ZIF-8 nanocrystals embedded inside the channels of macroporous anodic aluminum oxide membranes is reported. 1-D self-supported ZIF-8 superstructures are recovered through matrix dissolution.

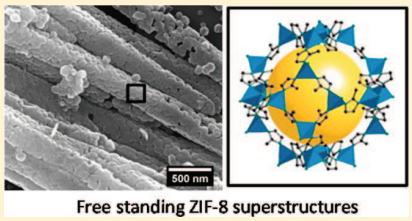

Metal−organic frameworks (MOFs) have been one of the most studied classes of porous solids over the past two decades.[1,2] Although most investigations concern crystalline solids, recent research has demonstrated that developing advanced architectures based on these porous coordination polymers could further expand their scope and facilitate their integration with other functional materials, hence imparting new functionalities.[3] For instance, porous coordination polymers have been associated with a wide range of organic and/or inorganic matrices,[4−6] leading to composites of importance in membrane technology, catalysis, and sensing.

Interest in MOF-superstructures, which result from the controlled assemblage of MOF-nanocrystals in 1-, 2-, and 3-D macrostructures, is much more recent.[7,8] Such materials are particularly appealing because they provide an opportunity to tune the properties of microporous solids by exerting control over crystal size or morphology and their macroscopic assemblages, rather than by modifying the coordination polymer itself.[8] MOF-superstructures such as capsules and microspheres[9−12] or 2D and 3D mesoscopic architectures have been obtained using soft or hard templates,[7,8] but the elaboration of related 1D assemblages is still rare.[13−15] Herein we report on an efficient preparation of 1D self-supported ZIF-8 superstructures formed by sequential growth of nanocrystals within the macroporous channels of commercial anodized aluminum oxide (AAO) membranes and subsequent matrix dissolution. The resulting objects, with a diameter of ca 200 nm and several micrometers in length, faithfully reproduce the shape induced by the inorganic template.

The zeolitic imidazolate framework ZIF-8 was chosen as a model system because of its outstanding chemical and structural robustness,[16] which is compatible with the conditions allowing the dissolution of the AAO matrix.[17] Using a dynamic step by step (SBS) percolation[18] of ZIF-8 reagents (i.e., zinc nitrate and 2-methylimidazole in methanol) through the AAO membranes allowed the growth of coordination polymer crystals over the whole length of the channels (Figure 1). However, two experimental parameters have to be imperatively satisfied to form the desired ZIF in a pure phase: (i) the membrane should be prefunctionalized by APTES (3-aminopropyltriethoxysilane); (ii) the zinc nitrate and 2-methylimidazole solutions filtered through the membrane must satisfy to a

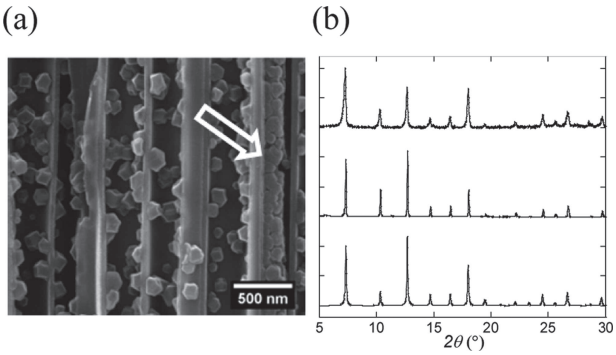

Figure 1. FESEM image (a) of the cross section of a membrane after 6 cycles of the optimized dynamic SBS treatment (Supporting Information is given in Figures S6 and S7) and PXRD patterns (b) calculated for ZIF-8 (bottom), experimental for bulk micro/nanocrystals of ZIF-8 (middle, see text) and for ZIF-8 composite membrane (top).

reagents ratio of 1:4, independently of their concentrations. The influence of the membrane functionalization and of the reagent ratio on the phase purity of ZIF-8 is illustrated in Figures S1 and S2 (SI). Moreover, while SBS procedures classically comprise a washing step between each reagent,[19] this was found to drastically reduce the efficiency of the formation of the MOF in the channels (see SI, Figures S3–S5 for additional information) and therefore was not applied in the present case.

In a typical experiment, $Zn(NO_3)_2$ (0.1 M in MeOH), 2-methylimidazole (0.4 M in MeOH), and MeOH were allowed to flow sequentially through the prefunctionalized membrane, each solution during 10 min, and this cycle was repeated six times (for details, see experimental section in SI). This procedure yields composite material with high and homogeneous load of ZIF-8 over the whole membrane thickness. The efficiency of this process can be attributed to the absence of any washing step between percolation of the reagents, which leads to partial mixing of the solutions ahead of the membrane. In these conditions, ZIF-8 crystal seeds are already formed before entering the membrane and then disseminated along the channels by the liquid flow. The formation of nanosized ZIF-8 crystals during the first minutes following the mixture of the reagent solutions was confirmed by diffusion light scattering (DLS, see Figure S8).

Scanning electron microscopy revealed that ZIF-8 forms well-shaped crystals of about 50–100 nm in size within the channels (Figure 1a and S6–S7). It must be stressed that these FESEM images only provide partial information on the actual filling of the channels. Indeed, cross section examination requires breaking the composite membrane, which results in expulsion of part of the crystals contained in the opened channels. A section of a channel with a full load of crystals can be seen in Figure 1a (arrowed) and this is further confirmed by the dissolution of the membrane (vide infra).

IR and PXRD experimental patterns obtained for these composite membranes fully agree with the ones found for bulk ZIF-8 prepared in same conditions (see Experimental Section and Figures S9 and S10 for details), and with the results reported in the literature.[16] ZIF-8 containing membranes were also characterized by N_2 adsorption isotherms recorded at 77 K. As expected, they display a mixed type I/type II isotherm,[20] in agreement with the coexistence of both micro- and macropores in the composite.[18] The BET surface area is increased up to 41 $m^2\ g^{-1}$ as compared with the starting commercial AAO matrix (ca. 7 $m^2\ g^{-1}$). The sharp adsorption in the low pressure range exclusively originates from the micropores of the ZIF-8, while the increase observed at high relative pressure with respect to the starting alumina membranes is attributed to intercrystal porosity (Figure S11a). The microporous surface area for the composite is estimated to be 30 $m^2\ g^{-1}$ by the α_s-plot (Figure S12a). The bimodal pore size distribution expected for ZIF-8[21] (i.e., pore sizes of 11.1 and 17.1 Å, respectively) is well evidenced by analyzing N_2 sorption isotherm using the Horvath–Kawazoe method (Figure S12b). Indeed, the step in the N_2 adsorption isotherm of ZIF-8, as evidenced on the semilog curve, reveals that the framework is not completely rigid and undergoes a structural transition upon N_2 exposure. This framework flexibility was previously attributed to the reorientation of imidazolate linkers during adsorption that enlarges the window size and allows N_2 to enter.[22] This feature shows that the alumina matrix does not modify the dynamic behavior of the ZIF-8 framework. Compared to a benchmark ZIF-8, which gave S_{BET} = 1830 $m^2\ g^{-1}$ (Figure S11b), the microporosity of the composite membranes corresponds to about 2.3 weight% of MOF. This value is slightly lower than the average content of ZIF-8 deduced from Zn and C elemental analyses performed on several composite membranes (see Table S1), suggesting that a fraction of the microporosity is hidden.

Immersing a ZIF-8 composite membrane in 2 M aqueous NaOH[17] led to a complete dissolution of the inorganic matrix in 20 min. The inertness of ZIF-8 in these conditions was confirmed with bulk MOF for which no modification of the PXRD patterns was found upon treatment with NaOH (see Figure S13). As can be seen in Figure 2a, for a partially dissolved membrane 1D superstructures of ZIF-8 are clearly visible in the remains of adjacent AAO channels, thus confirming the efficiency of the growth process. Bundles of ZIF-8 superstructures are obtained upon complete dissolution of the AAO membrane (Figure 2b and c). These superstructures show a diameter of ca. 200 nm, in agreement with the cross sections of the channels of the matrix. A reliable estimation of the actual length of the superstructures appears difficult by FESEM because they get broken during the transfer from the vial to the microscopy grids. However, several superstructures with a length of 10 to 15 μm have been observed (Figures 2d and S16), which remain still below the 60 μm of the membrane thickness.

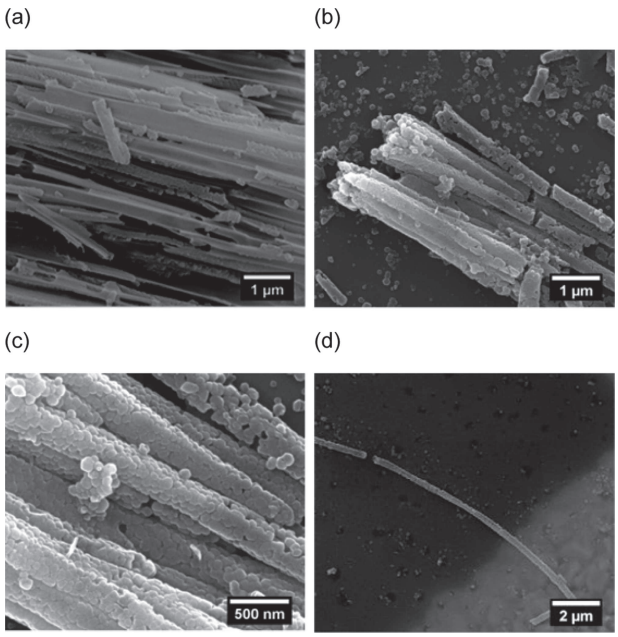

Figure 2. FESEM images for (a) the cross section of a ZIF-8 composite membrane after 10 min in 2 M NaOH and (b,c) ZIF-8 self-supported superstructure bundles recovered after membrane etching during 20 min in 2 M NaOH, and (d) a single free-standing ZIF-8 superstructure. Image (c) corresponds to an enlarged view of (b). Complementary information is supplied by Figures S14–S16.

Examination of superstructures at the single object level using high-resolution transition electronic microscopy (HRTEM, Figure 3a and b) confirmed that these assemblages are formed by intergrown crystals, whose sizes range from 60 to 110 nm. EDX spectra (Figure S17) revealed the presence of Zn, C, and N, in agreement with the chemical composition of ZIF-

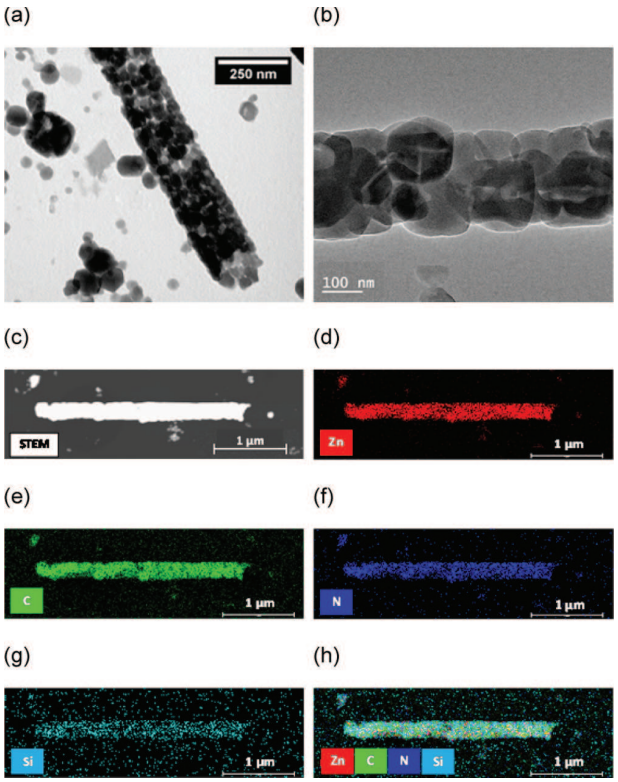

Figure 3. HRTEM images (a,b) for single free-standing ZIF-8 superstructures. STEM-HAADF image (c) and EDX maps (d–h) showing the spatial distribution of elements in ZIF-8 free-standing superstructures: (d) Zn map; (e) C map; (f) N map; and (g) Si map. Image (h) corresponds to the Zn + C + N + Si map. Complementary information is supplied by Figure S17.

8. The homogeneous distribution of this composition over a whole superstructure was confirmed by STEM mapping (Figure 3). The presence of silicon residues arising from the membrane functionalization with APTES were also evidenced at the superstructure periphery by using this technique.

Further evidence of the persistence of the ZIF-8 phase for these superstructures was obtained by RAMAN spectroscopy coupled to atomic force microscopy (AFM). As can be seen in Figure 4, the Raman spectrum recorded for a superstructure compares well with the one obtained for bulk ZIF-8. Finally, topography investigations of heights of objects by AFM led to a mean value of 170 nm and a profile in perfect agreement with the channel diameter for a membrane (ca. 200 nm), therefore indicating that the superstructures do not collapse when they are released from the matrix (Figures 4 and S18).

The gathered results show that 1-D superstructures of nanoporous ZIF-8 can be readily prepared by using commercial AAO membranes as sacrificial matrixes. Noteworthy, this is the first time that a hard-template assisted growth is successfully applied to the elaboration of 1D assemblages of MOF nanocrystals.[23,24] The resulting thread-like objects reproduce the shape of the templating channels, thus suggesting the possibility to tune their metrics through the choice of the commercial membranes' features or moving to calibrated homemade templates.[25] Interestingly, the growth of submicronic crystals of MOFs inside the channels of a macroporous commercial AAO membrane is also a particularly efficient way to prepare composite materials where the microporous solid is

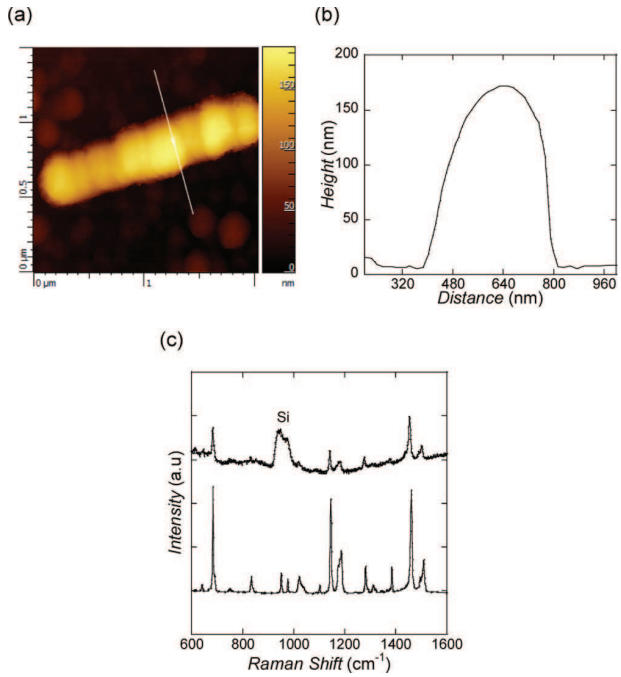

Figure 4. AFM-Raman combined measurements. (a) AFM image (tapping mode) for a single ZIF-8 superstructure deposited on a silicon wafer. (b) Height profile for the superstructure. (c) Raman spectra for bulk ZIF-8 (bottom) and for the considered free-standing ZIF-8 superstructure.

embedded in an inorganic protecting shell. Such composites can be of interest for other purposes. As far as ZIF-8 is concerned, experimental considerations such as membrane functionalization, reagent stoichiometry, and forced flow through the membrane channels are important parameters to allow growth of the MOF in a pure phase as nanocrystals over the whole membrane thickness.

■ ASSOCIATED CONTENT

Supporting Information

Experimental procedures, information on the role of the experimental conditions, N_2 adsorption isotherms, additional FESEM data, composition analyses. The Supporting Information is available free of charge on the ACS Publications website at DOI: 10.1021/acs.cgd.5b00687.

■ AUTHOR INFORMATION

Corresponding Authors

*E-mail: nans.roques@lcc-toulouse.fr

*E-mail: sutter@lcc-toulouse.fr.

Author Contributions

The manuscript was written through contributions of all authors. All authors have given approval to the final version of the manuscript.

Notes

The authors declare no competing financial interest.

■ ACKNOWLEDGMENTS

This work was supported by the French Agence Nationale pour la Recherche, under the project ANR-10-JCJC-0707 "HP-MOFs", by the University of Toulouse and the Région Midi-Pyrénées, under the project "MOFinMeAl", and by the

"Conseil Régional de Bourgogne" (programs PARI IME SMT8 and PARI II CDEA). The authors are grateful to V. Collière and M. Tassé (LCC−CNRS) for technical assistance in microscopy investigations.

REFERENCES

(1) Furukawa, H.; Cordova, K. E.; O'Keeffe, M.; Yaghi, O. M. *Science* **2013**, *341*, 1230444.
(2) Allendorf, M. D.; Stavila, V. *CrystEngComm* **2015**, *17*, 229−246.
(3) Shekhah, O.; Liu, J.; Fischer, R. A.; Woell, C. *Chem. Soc. Rev.* **2011**, *40*, 1081−1106.
(4) Qiu, S. L.; Xue, M.; Zhu, G. S. *Chem. Soc. Rev.* **2014**, *43*, 6116−6140.
(5) Stavila, V.; Talin, A. A.; Allendorf, M. D. *Chem. Soc. Rev.* **2014**, *43*, 5994−6010.
(6) Yao, J. F.; Wang, H. T. *Chem. Soc. Rev.* **2014**, *43*, 4470−4493.
(7) Carne-Sanchez, A.; Imaz, I.; Stylianou, K. C.; Maspoch, D. *Chem. - Eur. J.* **2014**, *20*, 5192−5201.
(8) Furukawa, S.; Reboul, J.; Diring, S.; Sumida, K.; Kitagawa, S. *Chem. Soc. Rev.* **2014**, *43*, 5700−5734.
(9) Ameloot, R.; Vermoortele, F.; Vanhove, W.; Roeffaers, M. B. J.; Sels, B. F.; De Vos, D. E. *Nat. Chem.* **2011**, *3*, 382−387.
(10) Carne-Sanchez, A.; Imaz, I.; Cano-Sarabia, M.; Maspoch, D. *Nat. Chem.* **2013**, *5*, 203−211.
(11) Pang, M.; Cairns, A. J.; Liu, Y.; Belmabkhout, Y.; Zeng, H. C.; Eddaoudi, M. *J. Am. Chem. Soc.* **2013**, *135*, 10234−10237.
(12) Hirai, K.; Reboul, J.; Morone, N.; Heuser, J. E.; Furukawa, S.; Kitagawa, S. *J. Am. Chem. Soc.* **2014**, *136*, 14966−14973.
(13) Yanai, N.; Sindoro, M.; Yan, J.; Granick, S. *J. Am. Chem. Soc.* **2013**, *135*, 34−37.
(14) Zhang, W.; Wu, Z.-Y.; Jiang, H.-L.; Yu, S.-H. *J. Am. Chem. Soc.* **2014**, *136*, 14385−14388.
(15) Pachfule, P.; Balan, B. K.; Kurungot, S.; Banerjee, R. *Chem. Commun.* **2012**, *48*, 2009−2011.
(16) Park, K. S.; Ni, Z.; Cote, A. P.; Choi, J. Y.; Huang, R.; Uribe-Romo, F. J.; Chae, H. K.; O'Keeffe, M.; Yaghi, O. M. *Proc. Natl. Acad. Sci. U. S. A.* **2006**, *103*, 10186−10191.
(17) Xiao, Z. L.; Han, C. Y.; Welp, U.; Wang, H. H.; Kwok, W. K.; Willing, G. A.; Hiller, J. M.; Cook, R. E.; Miller, D. J.; Crabtree, G. W. *Nano Lett.* **2002**, *2*, 1293−1297.
(18) Maksoud, M.; Roques, N.; Brandes, S.; Arurault, L.; Sutter, J.-P. *J. Mater. Chem. A* **2013**, *1*, 3688−3693.
(19) Shekhah, O.; Swaidan, R.; Belmabkhout, Y.; du Plessis, M.; Jacobs, T.; Barbour, L. J.; Pinnau, I.; Eddaoudi, M. *Chem. Commun.* **2014**, *50*, 2089−2092.
(20) Sing, K. S. W.; Everett, D. H.; Haul, R. A. W.; Moscou, L.; Pierotti, R. A.; Rouquerol, J.; Siemieniewska, T. *Pure Appl. Chem.* **1985**, *57*, 603−619.
(21) Lu, G.; Li, S.; Guo, Z.; Farha, O. K.; Hauser, B. G.; Qi, X.; Wang, Y.; Wang, X.; Han, S.; Liu, X.; DuChene, J. S.; Zhang, H.; Zhang, Q.; Chen, X.; Ma, J.; Loo, S. C. J.; Wei, W. D.; Yang, Y.; Hupp, J. T.; Huo, F. *Nat. Chem.* **2012**, *4*, 310−316.
(22) Fairen-Jimenez, D.; Moggach, S. A.; Wharmby, M. T.; Wright, P. A.; Parsons, S.; Dueren, T. *J. Am. Chem. Soc.* **2011**, *133*, 8900−8902.
(23) Note: An earlier attempt to shape the Zn/benzenedicarboxylate porous coordination polymer MOF-5 by AAO membranes has been reported (see ref 24) but this coordination compound was shown to be highly unstable in the acidic condition required for dissolution of the aluminum oxide matrix.
(24) Huang, L.; Wang, H. H.; Chen, J.; Wang, Z.; Sun, J.; Zhao, D.; Yan, Y. *Microporous Mesoporous Mater.* **2003**, *58*, 105−114.
(25) Ciambelli, P.; Arurault, L.; Sarno, M.; Fontorbes, S.; Leone, C.; Datas, L.; Sannino, D.; Lenormand, P.; Du Plouy, S. L. B. *Nanotechnology* **2011**, *22*, 265613.